Colloid Adsorption onto Responsive Membranes

Rita S. Dias and Per Linse
Physical Chemistry 1, Center for Chemistry and Chemical Engineering, Lund University, Lund, Sweden

ABSTRACT The adsorption of colloids of varying sizes and charges onto a surface that carries both negative and positive charges, representing a membrane, has been investigated using a simple model employing Monte Carlo simulations. The membrane is made of positive and negative charges (headgroups) that are allowed to move along the membrane, simulating the translational diffusion of the lipids, and are also allowed to protrude into the solution, giving rise to a fluid and soft membrane. When an uncharged colloid is placed in the vicinity of the membrane, a short-range repulsion between the colloid and the membrane is observed and the membrane will deflect to avoid coming into contact with the colloid. When the colloid is charged, the membrane response is twofold: the headgroups of the membrane move toward the colloid, as if to partly embrace it, and the positive headgroups of the membrane approach the oppositely charged colloid, inducing the demixing of the membrane lipids (polarization). The presence of protrusions enhances the polarization of the membrane. Potential of mean force calculations show that protrusions give rise to a more long-range attractive colloid-membrane potential which has a smaller magnitude at short separations.

INTRODUCTION

Adsorption of biomacromolecules onto lipid membranes is of great biological and technological importance. Some examples are protein-membrane interactions in cells, DNA packaging in viral capsids with internal lipid membranes (1), DNA adsorption onto liposomes for lipoplex preparation in gene delivery, and the interaction of such complexes with cell membranes.

This has prompted a number of experimental, theoretical, and simulation studies using various model systems. However, lipid membranes are not static, flat homogeneous structures, but present a large number of dynamic modes. The individual lipid molecules in the bilayer undergo lateral diffusion, wobbling, rotations, and vertical excursions (protrusions) out of the bilayer. This will naturally have an impact on 1), the structure of the bilayer itself, well described as a liquid but possessing a structured interface with specific elastic and mechanical properties, and 2), the interactions between the bilayer and biomacromolecules, such as DNA and proteins.

When a membrane is in its fluid state, the lipids have a relatively fast lateral diffusion and are, in principle, responsive when a charged object approaches. The domain formation (demixing) of the lipids has been observed experimentally upon the adsorption of DNA molecules on cationic membranes (2,3) and the adsorption of peptides on giant unilamellar vesicles (4).

Accordingly, the number of theoretical and computational studies on the interaction of proteins (5–9) and polyectrolytes (10–12) with fluid lipid membranes has increased in recent years. It was observed that the adsorption of macromolecules induces the demixing of the lipids in the membrane and that the demixing, in turn, increases the binding energy of the macromolecule to the membrane. Furthermore, it was observed that the demixing of the lipids (or membrane polarization) affects the adsorption isotherm of proteins and protein-protein interactions (5,7,9) and also induces some degree of compaction of an adsorbed polyelectrolyte (11).

As mentioned above, besides being fluid, membranes are also soft structures. This is partially due to protrusions of the thermally excited lipids out of the bilayer. These are believed to be of biological significance, and are suggested to be the source of the short-range repulsion forces present between amphiphilic surfaces (13–15). It has also been proposed that the protrusion of single lipid molecules out of the bilayer plane is directly related to the activity of phospholipase A_2 on lipid bilayers (16,17).

The fact that the membrane is flexible influences the interaction with macromolecules, a typical example being the endocytosis of viruses and bioparticles into the cell. Even though endocytosis is driven by receptor-mediated mechanisms, the biophysical properties of cell membranes are probably of importance, since the process is dependent on, for example, the particle size and cell rigidity (see (18,19) and references therein).

A number of theoretical studies have been conducted on the interaction of colloids (20–23) and rodlike polyions (24) with flexible membranes. These studies involve the bending of the membrane in the presence of macromolecules, and effects such as colloid size and charge, salt, and charge density and flexibility of the membrane have been considered. Computer simulations involving the interaction of soft membranes with macromolecules are still rare, and most of them deal with the inclusion of transmembrane proteins in the membrane (25–28). Other interesting studies have been

Submitted August 2, 2007, and accepted for publication December 3, 2007.

Address reprint requests to Rita S. Dias, Physical Chemistry 1, Center for Chemistry and Chemical Engineering, Lund University, S-221 00 Lund, Sweden. Tel.: 46-46-2228148; Fax: 46-46-2224413; E-mail: Rita.Dias@fkem1.lu.se.

Editor: Angel E. Garcia.

0006-3495/08/05/3760/09 $2.00

doi: 10.1529/biophysj.107.118877

reported that deal with the adhesion of a particle to, and its engulfment by, a vesicle (29), and the aggregation and vesiculation of membrane proteins arising from the curvature of the membrane (30).

The aim of this work was to study 1), how a fluid membrane carrying equal amounts of positively and negatively charged lipids interacts with a colloid; and 2), how the membrane responds to this interaction. In particular, we used a coarse-grained model to investigate how the interaction depends on the degrees of freedom of the individual lipids. The main findings are that 1), with an uncharged colloid near the membrane, a short-range repulsion arises due to the protrusion modes, and the membrane deflects away from the colloid; and 2), with a charged colloid near the membrane, an attractive interaction appears between the membrane and the colloids that originates from an in-plane demixing of the lipids and a displacement of the lipids toward the colloid as if to embrace it. The effect of the lipid protrusions is to increase the lipid demixing and to make the membrane-colloid interaction more long-range but smaller in magnitude at short separations.

All model systems are simplifications of real systems. In this initial work, we 1), restrict the lipids so that their long axis is parallel to the surface normal, and hence suppress splay deformation; 2), neglect surface charge polarization at the lipid and macroion surfaces; and 3), consider only net neutral surfaces. Notwithstanding, we believe that it is important to understand this model system before introducing further complexity.

MODEL AND METHOD

Model

A simple model has been adopted to describe the adsorption of a colloid from solution onto a membrane composed of cationic and anionic lipids. Important components of the model include 1), in-plane translational mobility of the lipids (demixing); 2), out-of-plane translational mobility of the lipids (protrusions); and 3), an explicit description of all charged species.

We use a membrane model, of which many of its features originate from a previous study (31). Briefly, the model contains one leaflet of a membrane. The membrane is composed of N_{lip} lipids, each having a headgroup and a tail. The headgroup is represented by a charged hard sphere, and the tail by a rectangular parallelepiped. The tails are oriented parallel to the normal of the membrane, and the headgroup is in hard-sphere contact with its tail. The headgroups have a local and a long-range translational mobility, the latter through the exchange of positions of oppositely charged lipids. The protrusions of individual lipids into the water solution lead to an exposure of hydrophobic tails to water. The membrane model is illustrated in Fig. 1 *A*.

The colloid and its monovalently charged counterions are represented by charged hard spheres, characterized by their radius and charge. The investigated system is electroneutral. The solvent enters the model only through its relative permittivity.

Consider a rectangular box with lengths $L_{\mathrm{x}} = L_{\mathrm{y}} = 200$ Å and $L_{\mathrm{z}} = 600$ Å. Periodic boundary conditions are applied in the x and y directions. The average position of the headgroups $\langle z_{\mathrm{h}} \rangle$ is localized at $z = 0$ Å, whereas a hard wall is placed at $z = z_{\mathrm{wall}} = 400$ Å. The extension in the z direction available for the colloid and its counterions is thus restricted by $\langle z_{\mathrm{h}} \rangle$ and z_{wall}. Thus, formally we investigate a system with a finite colloid concentration; however, we argue that the membrane is sufficiently large to make the results representative for adsorption of a single colloid.

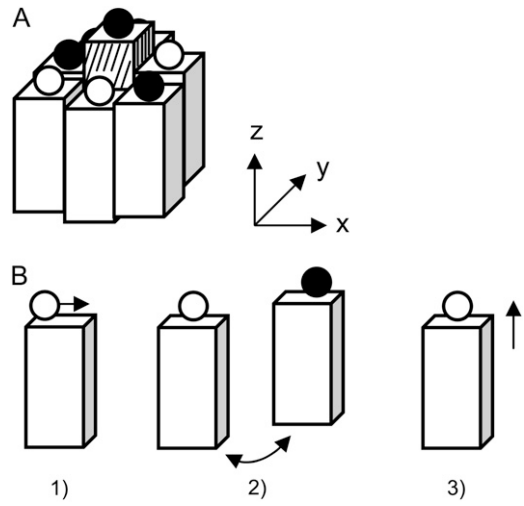

FIGURE 1 (*A*) Perspective illustration of the membrane showing the lipids represented by charged hard spheres and parallelepipeds, hydrophobic-water contact areas (*shaded surfaces*), and the external coordinate system. (*B*) Illustration of the three types of lipid trial displacements: 1), local headgroup trial displacement, 2), lipid exchange, and 3), lipid-protrusion trial displacement.

In more detail, the total potential energy, U, of the system can be expressed as a sum of five contributions according to

$$U = U_{\mathrm{el}} + U_{\mathrm{hs}} + U_{\mathrm{h-t}} + U_{\mathrm{prot}} + U_{\mathrm{ext}}. \tag{1}$$

The electrostatic potential energy, U_{el}, is given by

$$U_{\mathrm{el}} = \sum_{\mathrm{i<j}} \frac{Z_{\mathrm{i}} Z_{\mathrm{j}} e^2}{4\pi\varepsilon_0\varepsilon_{\mathrm{r}}} \frac{1}{r_{\mathrm{i,j}}}, \tag{2}$$

where the summation extends over pairs of spherical particles (lipid headgroups, colloid, and simple ions), with Z_{i} and R_{i} denoting the valence and radius, respectively, of particle i; $r_{\mathrm{i,j}} = |\mathbf{r}_{\mathrm{j}} - \mathbf{r}_{\mathrm{i}}|$ the distance between particles j and i; e representing the elementary charge, ε_0 the permittivity of vacuum; and ε_{r} the relative permittivity of the solvent. The simplification of a uniform relative permittivity of the system implies that the charge polarization at the lipid and macroion surfaces is neglected. The hard-sphere potential, U_{hs}, is given by

$$U_{\mathrm{hs}} = \sum_{\mathrm{i<j}} u^{\mathrm{hs}}_{\mathrm{i,j}}(r_{\mathrm{i,j}}) + \sum_{\mathrm{t,i}} u^{\mathrm{hyd}}_{\mathrm{t,i}}(\mathbf{r}_{\mathrm{t}}, \mathbf{r}_{\mathrm{i}}), \tag{3}$$

where the first summation extends over all pairs of spherical particles with

$$u^{\mathrm{hs}}_{\mathrm{i,j}}(r_{\mathrm{i,j}}) = \begin{cases} \infty, & r_{\mathrm{i,j}} < R_{\mathrm{i}} + R_{\mathrm{j}} \\ 0, & r_{\mathrm{i,j}} \geq R_{\mathrm{i}} + R_{\mathrm{j}} \end{cases}, \tag{4}$$

and the second summation describes the interaction between tail t and particle i with

$$u^{\mathrm{hyd}}_{\mathrm{t,i}}(\mathbf{r}_{\mathrm{t}}, \mathbf{r}_{\mathrm{i}}) = \begin{cases} \infty, & |x_{\mathrm{i}} - x_{\mathrm{t}}| < (R_{\mathrm{i}} + l/2) \ \text{and} \\ & |y_{\mathrm{i}} - y_{\mathrm{t}}| < (R_{\mathrm{i}} + l/2) \ \text{and} \\ & z_{\mathrm{i}} < z_{\mathrm{t}} + R_{\mathrm{i}} \\ 0, & \text{else} \end{cases}, \tag{5}$$

where $\mathbf{r}_{\mathrm{t}} = (x_{\mathrm{t}}, y_{\mathrm{t}}, z_{\mathrm{t}})$ denotes the center of the quadratic surface of tail t, to which its headgroup is attached, and l the edge length of the quadratic cross

section of a tail. Furthermore, the intralipid headgroup-tail potential energy, $U_{\text{h-t}}$, is given by

$$U_{\text{h-t}} = \sum_{\text{l}=1}^{\text{N}_{\text{lip}}} u_{\text{h-t}}, \tag{6}$$

where the summation extends over all lipids with

$$u_{\text{h-t}} = \begin{cases} \infty, & |x_{\text{i}} - x_{\text{t}}| > l/2 \text{ or } |y_{\text{i}} - y_{\text{t}}| > l/2 \text{ or } z_{\text{i}} \neq z_{\text{t}} + R_{\text{i}} \\ 0, & \text{else} \end{cases}, \tag{7}$$

where $\mathbf{r}_{\text{i}}$ and $\mathbf{r}_{\text{t}}$ denote the coordinates of the headgroup and the tail residing in the same lipid. The protrusion potential energy, U_{prot}, was evaluated according to

$$U_{\text{prot}} = \sum_{\text{t}=1}^{N_{\text{lip}}} \gamma A_{\text{t}}, \tag{8}$$

where the summation extends over all the lipid tails, γ is the surface tension, and A_{t} the area of tail t exposed to water (see Fig. 1 *A*) given by

$$A_{\text{t}} = l \sum_{\text{t}'=1}^{4} (z_{\text{t}} - z_{\text{t}'})\Theta(z_{\text{t}} - z_{\text{t}'}), \tag{9}$$

with t' denoting the nearest-neighbor tails of tail t and $\Theta(x)$ the Heavside step function with the properties $\Theta = 0$ for $x < 0$, and $\Theta = 1$ for $x \geq 0$. Here, we have used $\gamma = 18$ mJ m^{-2} (32–35). Finally, the confining external potential energy, U_{ext}, is given by

$$U_{\text{ext}} = \sum_{\text{i}} u_{\text{ext}}(z_{\text{i}}), \tag{10}$$

where the summation extends over all the spherical particles with

$$u_{\text{ext}}(z_{\text{i}}) = \begin{cases} \infty, & z_{\text{i}} \geq z_{\text{wall}} \\ 0, & z_{\text{i}} < z_{\text{wall}} \end{cases}. \tag{11}$$

For simplicity, the same hard-sphere radius $R_{\text{i}} = 2$ Å has been used for the headgroups and the simple ions. Throughout, an equal number of cationic and anionic lipids have been used; hence, the net charge of the membrane with charged lipids is always zero. With $N_{\text{lip}} = 1024$ lipids and fixed values of L_{x} and L_{y}, the membrane is incompressible with a hard-sphere area fraction $1024\pi R_{\text{h}}^2/L_{\text{x}}L_{\text{y}} = 0.32$. Colloids with radius $R_{\text{c}} = 10$ Å and charges $Z_{\text{c}} = 0, -10$, and -20, as well as radius $R_{\text{c}} = 20$ Å and charges $Z_{\text{c}} = -20, -40$, and -60 have been examined. The colloid with $R_{\text{c}} = 10$ Å and $Z_{\text{c}} = -20$ will be referred to as the reference colloid. Throughout, $T = 298$ K and $\varepsilon_{\text{r}} = 78.4$ have been used.

In addition, complementary systems with 1), a single membrane, 2), lipids with uncharged headgroups, or 3), lipids with restricted degrees of freedom have been investigated.

Simulation details

All Monte Carlo simulations were performed in the canonical ensemble, employing the standard Metropolis algorithm (36). The long-range electrostatic interactions were handled using the Ewald summation with a recent extension to slab geometry (37). This extension motivated the use of a simulation box exceeding the distance available in the z direction.

Lipids were subjected to three types of trial moves: 1), a trial transverse displacement of a headgroup with respect to its stationary tail; 2), exchange of the positions of two lipids; and 3), lipid trial displacement parallel to the membrane normal. These trial moves are illustrated in Fig. 1 *B*. The average z coordinate of the headgroups $\langle z_{\text{h}} \rangle$ was fixed at $z = 0$ to avoid a drift of the membrane in the z direction. Throughout, the colloid was fixed at the membrane-colloid surface-to-surface separation, s, measured from a headgroup located at $\langle z_{\text{h}} \rangle = 0$. The simple ions were subjected to simple translational moves.

Since we are using a lattice to describe the membrane, the results become weakly dependent on the precise colloid position in the xy plane. To reduce this grid effect, all systems were calculated three times, where the x and the y positions of the colloid were varied within one of the squares of the grid.

Each simulation included an equilibration of at least 2×10^5 trial moves per particle followed by a production run of at least 5×10^5 trial moves per particle. Statistical uncertainties were evaluated by dividing the total simulation into subbatches. All the simulations were performed using the simulation package MOLSIM (38).

Properties examined

In this investigation, we have determined the interaction between the membrane and the colloid, as well as structural aspects of the membrane including the out-of-plane headgroup density profile and in-plane headgroup polarization.

The membrane-colloid interaction was determined by calculation of the potential of mean force (pmf), U_{pmf}, acting on the colloid at different membrane-colloid separations, s. The mean force, F, operating on the colloid, c, and projected on the z axis was calculated according to

$$F(s) = \sum_{\text{i}\neq\text{c}}^{\text{N}} \langle -\nabla_{\text{r}_{\text{c,i}}} U_{\text{c,i}}(r_{\text{c,i}}) \rangle, \tag{12}$$

where $U_{\text{c,i}}$ denotes the potential energy between the colloid and particle i (lipid headgroup, lipid tail, and simple ions) at the separation $r_{\text{c,i}}$, $N = N_{\text{lip}} + |Z_{\text{c}}|$ is the number of particles, and $\langle \ldots \rangle$ indicates an ensemble average. The electrostatic and hard-core contributions to the force were handled separately (39). $F(s) > 0$ implies a repulsive and $F(s) < 0$ an attractive mean force. The potential of mean force between the membrane and the colloid, U_{pmf}, is related to the mean force according to

$$U_{\text{pmf}}(s) = -\int_{\infty}^{s} F(r)dr, \tag{13}$$

where the convention $U_{\text{pmf}}(s) \to 0$ as $s \to \infty$ has been used. The integral was determined numerically using the trapezoidal rule.

RESULTS AND DISCUSSION

Single membrane

Before examining the membrane-colloid system, a brief characterization of single membranes composed of lipids possessing 1), uncharged or 2), charged headgroups will be given. We remind the reader that the latter membrane contains an equal number of lipids having cationic and anionic headgroups and has a zero net charge.

Fig. 2 *A* shows the headgroup number density as a function of the z direction, i.e., the dispersion of the headgroup location perpendicular to the membrane. The dispersions of the two systems are essentially Gaussian. The width of the Gaussian dispersion is 3.01 Å for uncharged headgroups (*dashed curve*) and 2.86 Å for charged headgroups (*solid curve*). Hence, the width with the charged headgroups is slightly smaller, which we attribute to the cohesive nature of the electrostatic interaction of an electroneutral system. A snapshot of the system with charged headgroups is displayed in Fig. 2 *B*. As expected, the cationic and anionic headgroups

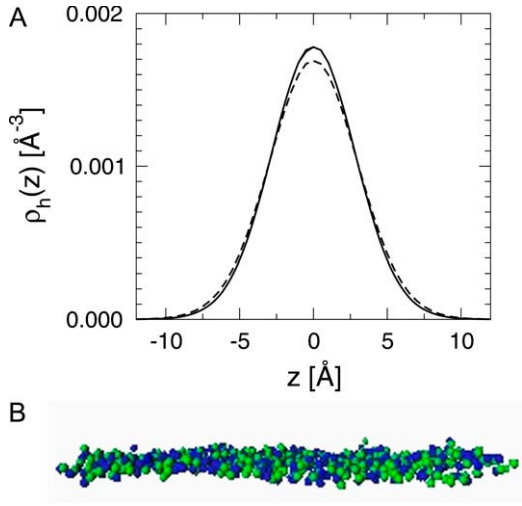

FIGURE 2 (*A*) Headgroup number density $\rho_h(z)$ as a function of the z coordinate for uncharged (*dashed curve*) and charged (*solid curve*) lipids. (*B*) Snapshot illustrating the location of the headgroups of charged lipids. Green and blue represent the positively and negatively charged headgroups, respectively.

essentially form a two-dimensional layer and the headgroups are well mixed. Nevertheless, individual lipids protrude into the aqueous solutions and membrane undulations of different wavelengths are present.

The capillary wave theory provides a prediction of the magnitude of the membrane fluctuations of different wavelengths. In the absence of gravity, the mean square of the capillary amplitude is given by (40)

$$\langle z^2 \rangle = \frac{kT}{4\pi\gamma} \ln\left(\frac{L_{\min}}{L_{\max}}\right), \tag{14}$$

where k is the Boltzmann constant, $L_{\min}$ the lower wavelength limit (of the order of a molecular diameter), and $L_{\max}$ the upper wavelength, determined by the size of the surface. With the use of $T = 298$ K, $L_{\min} = 6.35$ Å, $L_{\max} = 200$ Å, and $\gamma = 18$ mJ m^{-2}, capillary wave theory predicts $\langle z^2 \rangle^{1/2} = 2.5$ Å. This prediction is in good agreement with the dispersion of our model system.

Experimental electron density profiles from diffraction experiments of membranes composed of DOPC, DMPC, DLPC, and DPPC lipids have given the dispersions 2.5, 3.2, 3.3, and 3.75 Å (41–43), respectively. Computer simulations of various models have predicted dispersions of the headgroup location ranging from 1.7 to 4.5 Å (31,44–49).

Membrane-colloid systems

Membrane with uncharged lipids

To better understand the effect of the lipid charges, the interaction between a membrane with uncharged lipids and colloids with radius $R_c = 10$ Å and different charges will be given first.

Fig. 3 shows the potential of mean force U_{pmf} as a function of the membrane-colloid surface-to-surface separation for an uncharged colloid ($Z_c = 0$) and for a charged colloid ($Z_c = -20$) with its counterions. Independent of the colloid charge, the membrane-colloid interaction is purely repulsive. In the case of the uncharged colloid, the onset of the repulsion appears at $s \approx 5$ Å, which is in excellent agreement with the dispersion of the headgroup locations for an unperturbed membrane. At $s = 0$, the potential of mean force is $1.5kT$; hence, the free energy cost involved when the colloid surface penetrates to the center of the membrane is still moderate. The lipid protrusions in a membrane have long been considered to be the reason for the short-range repulsion observed between lipid bilayers (13–15). Clearly, the same mechanism is the cause of the repulsion between a membrane and a small colloid.

When the colloid is charged, the potential of mean force becomes 1), more long- range, and 2), greater in magnitude at short separations. This repulsion originates from the presence of the colloid's counterions. Far from the membrane, the distribution of the counterions around the colloid is spherically symmetric, and due to the electrostatic colloid-counterion attraction, a large fraction of the counterions are accumulated near the colloid (39). When the colloid is close to the membrane, the distribution of the counterions around the colloid becomes perturbed, giving rise to the additional effective membrane-colloid repulsion.

Membrane with charged lipids

We will continue by examining various properties of systems with a colloid near a net neutral membrane composed of charged lipids. Systems of lipids with full degrees of freedom (in-plane and out-of-plane lipid mobility) will be considered first, followed by a brief investigation of the effect of decomposing the degrees of freedom of the lipids.

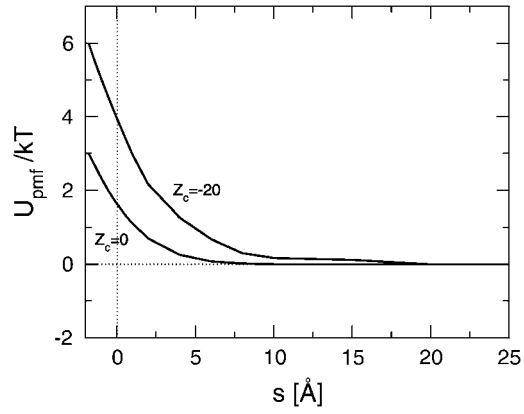

FIGURE 3 Reduced potential of mean force, $U_{pmf}(s)/kT$, as a function of the membrane-colloid separation, s, for uncharged lipids and colloids with radius $R_c = 10$ Å and the indicated charge.

Lipids with full degrees of freedom. Fig. 4 shows the potential of mean force between the membrane and colloids with radius $R_c = 10$ Å and charges $Z_c = 0, -10$, and -20. When the colloid is uncharged, the potential of mean force is repulsive and nearly identical to the one corresponding to the case with uncharged lipids and an uncharged colloid. This observation is consistent with the near identical z-dispersions for a membrane composed of uncharged and one composed of charged lipids (Fig. 2). However, when the colloid is charged, an attractive potential of mean force appears, which extends up to a separation of ≈20 Å. The minimum of the potential of mean force appears at $s \approx 3$ Å. The strength of the attraction increases with increasing colloidal charge. Under the conditions applied here, the depth of the attractive potential minimum increases linearly with increasing colloidal charge at a rate of $\approx kT/2$ per colloidal charge.

We will now examine the structural response of the membrane to a nearby colloid. Fig. 5 displays the average z-position of the headgroups as a function of the in-plane distance, ρ, between the headgroup and the normal to the membrane that intersects with the center of the colloid, at the membrane-colloid separation $s = 1.4$ Å. A quarter of the colloid and half of a headgroup drawn to scale are also displayed in Fig. 5 to illustrate the spatial arrangement. The separation selected corresponds to $U_{pmf} = 1kT$ for the uncharged colloid ($Z_c = 0$) and $-9kT$ for the charged colloid ($Z_c = -20$).

When the colloid is uncharged, a deflection of the membrane away from the colloid appears (Fig. 5 *A*). The maximal deflection occurring at $\rho = 0$ is 2.1 Å and the deflection increases to 2.4 Å when the colloid radius is increased to $R_c = 20$ Å. The deflection extends radially to $\rho \approx 30$ Å. The membrane deflection and the near absence of direct membrane-colloid contact are clearly visible in the inset. The reason for the deflection and its fairly large in-plane extension is that the presence of the colloid suppresses protrusion fluctuations. This suppression reduces the membrane entropy. The entropy loss becomes smaller upon deflection, which hence regains some of the protrusion fluctuations. However, coupled with the deflection, there is an increase of the water-tail contact area and, therefore, an associated interfacial free energy. Hence, the magnitude of the deflection is regulated by a membrane entropy-interface energy balance. The increased membrane deflection appearing for the larger colloid is due to the larger number of lipids that are affected.

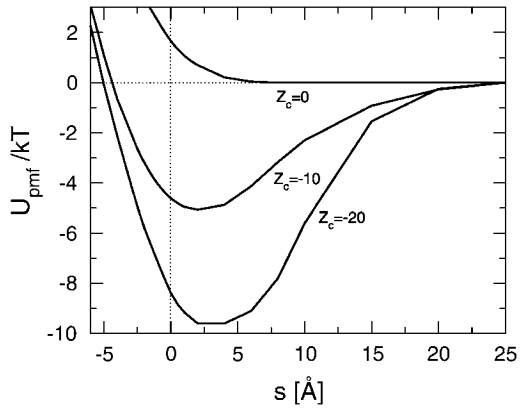

FIGURE 4 Reduced potential of mean force, $U_{pmf}(s)/kT$, as a function of the membrane-colloid separation, s, for charged lipids and colloids with radius $R_c = 10$ Å and the indicated charge.

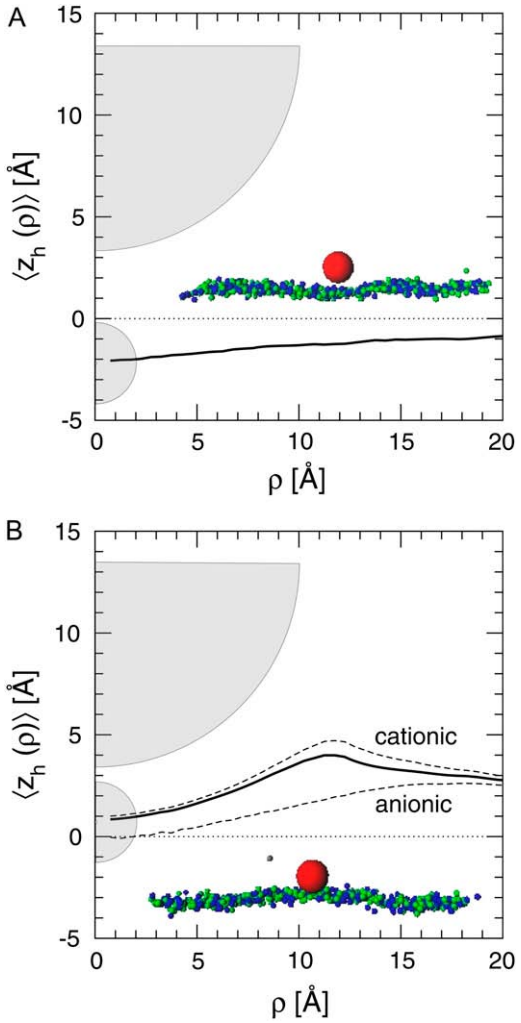

FIGURE 5 Average z-position of the headgroups (*solid curves*) as a function of the in-plane distance from the center of (*A*) an uncharged ($Z_c = 0$) and (*B*) a charged colloid ($Z_c = -20$) with radius $R_c = 10$ Å placed at the membrane-colloid separation $s = 1.4$ Å. The average z-position in the absence of colloid (*dotted line*), as well as a quarter of the colloid and half a lipid headgroup drawn at scale, are also shown. In *B*, the average z-positions of the cationic and anionic headgroups are also given (*dashed curves*). (*Insets*) Snapshots of the systems, where red is the colloid and green and blue are the positively and negatively charged headgroups, respectively.

The structural response of the membrane becomes very different when the colloid is charged. Now, 1), the headgroups are displaced toward the colloid; and 2), the displacement of the cationic headgroups is larger than that of the anionic ones

(Fig. 5 *B*). In fact, the headgroups partly embrace the colloid. The inset illustrates the headgroup-colloid contact and the partial embracement. Obviously, the attractive electrostatic interaction between the negatively charged colloid and the cationic headgroups is the cause of this drastically different behavior.

What is the membrane response at different membrane-colloid separations? Fig. 6 *A* displays the average *z*-position of the headgroups as a function of ρ for $s = 1.4$–13.2 Å for the reference colloid, the largest separation still corresponding to an attractive potential of $\approx 4kT$. Starting with $s = 1.4$ Å, as discussed previously, an increase of the membrane-colloid separation is followed by a displacement of the headgroups near the colloid toward the colloid. At $s = 5.3$ Å, the partial embracement still remains, whereas at $s = 9.3$ Å essentially only a point contact remains. The largest lipid out-of-plane displacement appears at $s \approx 11.3$ Å, and at larger membrane-colloid separations, the lipids do not adhere to the colloid any more. Some snapshots illustrating this behavior are shown in Fig. 6 *B*. Thus, for an appreciable variation of the membrane-colloid separation, the flexibility of the membrane enables headgroups to partially embrace the colloid.

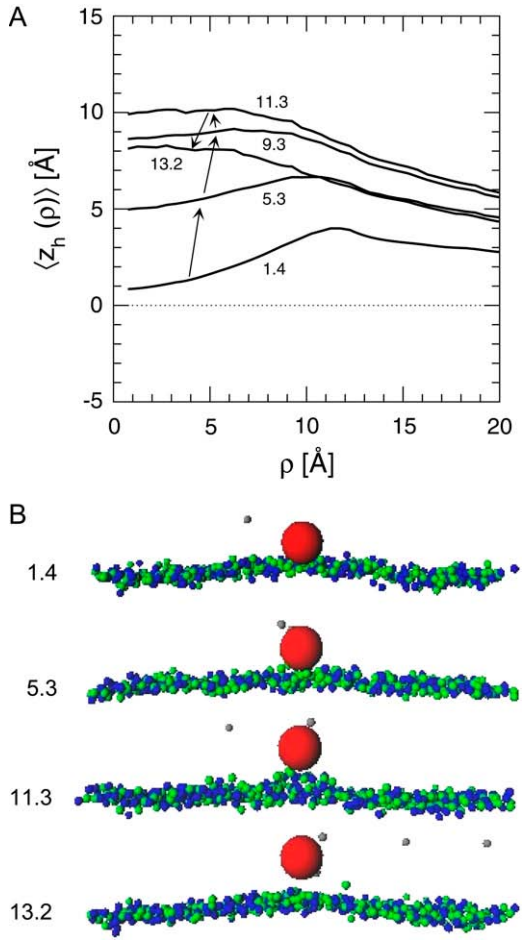

FIGURE 6 (*A*) Average *z*-position of the headgroups as a function of the in-plane distance from the center of the colloid for the reference colloid at the indicated membrane-colloid separations (Å). (*B*) Snapshots at the indicated colloid-membrane separation (Å). Red is the colloid and green and blue are the positively and negatively charged headgroups, respectively.

Fig. 7 shows $\langle z_h(\rho) \rangle$ at $\rho = 0$ versus s for the reference colloid (*solid curve*). The ability of the headgroup to locally adapt its out-of-plane location to the position of the colloid up to a well determined membrane-colloid separation, s_{max}, is observed. At $s = s_{max}$, the increased free energy cost associated with the increased water-tail surface matches the gain in the electrostatic energy. In a fairly small separation interval, the membrane snaps off the colloid. Table 1 summarizes s_{max} for other systems investigated. It is seen that s_{max} increases with the colloid charge at constant colloid size and decreases with increasing colloid size at constant colloid charge. Moreover, there is a lower threshold of the electrostatic interaction (represented by the colloidal charge) needed to have lipid-colloid contact at finite membrane-colloid separation ($s > 0$).

In addition to the out-of-plane dispersion of the headgroup locations, an in-plane polarization of the lipids takes place. We define the relative surface charge polarization $\sigma_r(\rho)$ as the surface charge density $\sigma(\rho)$ divided by the surface charge density for a surface with cations only, σ_{max}. Fig. 8 displays the relative surface charge polarization $\sigma_r(\rho)$ as a function of ρ at different membrane-colloid separations for the reference colloid. It is clear that near the colloid an appreciable in-plane charge polarization appears. At $s = 1.4$ Å, $\sigma_r(\rho = 0) \approx 0.8$, i.e., there is a 4:1 ratio favoring cationic headgroups. The excess of positive headgroups extends to $\rho \approx 30$ Å. In our model, with a finite-sized membrane in the canonical ensemble, the remaining membrane possesses a slightly negative charge to preserve its charge neutrality. At separation $s =$ 9.3 Å, 1), there is a slight increased favor of cationic headgroups in the vicinity of the colloid, but 2), spatial extension of the region with a positive net charge is smaller, making the integrated excess of positive charge smaller.

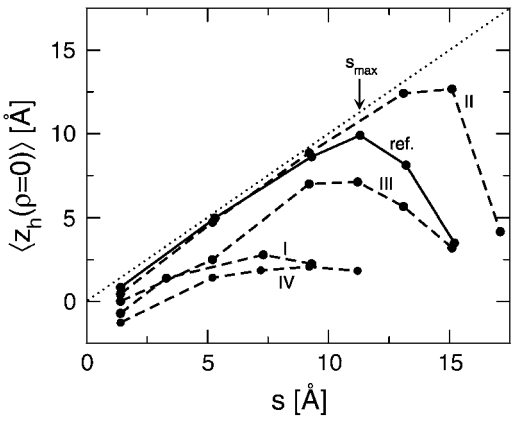

FIGURE 7 Average *z*-position of the headgroups at $\rho = 0$ as a function of the colloid-membrane separation, *s*, for different colloids. The condition for colloid-lipid close contact is also given (*dotted line*).

TABLE 1 Membrane-colloid separation at which the colloid desorbs from the membrane, s_{max}, maximal extension of the region with positive net charge, ρ', and local excess charge, Z_{ex}

Colloid	R_c (Å)	Z_c	s_{max} (Å)	ρ' (Å)*	Z^*_{ex}
Reference	10	−20	11.3	34.2	19.0
I	10	−10	7.3	38.2	9.1
II	20	−60	15.1	39.7	22.5
III	20	−40	11.2	43.7	15.3
IV	20	−20	9.2	48.2	8.2

*Values given are for $s = 1.4$ Å.

The excess surface charge of the region with a positive net charge, Z_{ex}, was calculated according to

$$Z_{ex} = 2\pi \int_0^{\rho'} \sigma(\rho)\rho d\rho, \quad (15)$$

where ρ' is the radial distance at which the average local charge of the membrane becomes negative. At increasing separation, the excess surface charge decreases ($Z_{ex} = 19.0$, 18.2, 15.7, and 3.8 at $s = 1.4$, 5.3, 11.3, and 21.2 Å, respectively). Table 1 summarizes the values obtained for ρ' and Z_{ex} at $s = 1.4$ Å for other studied systems. In the same fashion as the out-of-plane displacement, the in-plane polarization increases upon increasing colloid charge and decreases upon increasing colloid radius.

Hence, as the colloid approaches the membrane, in addition to the out-of-plane response, a considerable in-plane charge polarization appears.

Lipids with partial degrees of freedom. We will now decompose the two degrees of freedom of the lipids to assess their contribution to the membrane-colloid interaction. Fig. 9 shows the potential of mean force curves for the reference colloid at four different conditions: 1), in-plane and out-of-plane lipid mobility (labeled ρz); 2), in-plane lipid mobility only (ρ); 3), out-of-plane lipid mobility only (z); and 4), no lipid mobility (*two dashes*). In all four cases, the headgroups have a local mobility with respect to their tails. In the cases of no in-plane lipid mobility, the cationic and anionic lipids were arranged in a checkerboard pattern.

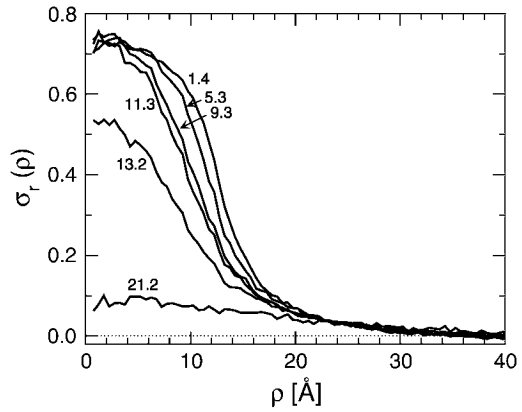

FIGURE 8 Relative surface charge polarization $\sigma_r(\rho)$ as a function of ρ for the reference colloid at the indicated membrane-colloid separations (Å).

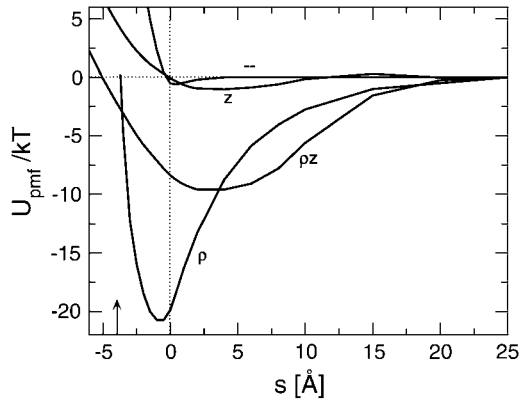

FIGURE 9 Reduced potential of mean force as a function of the membrane-colloid separation for the reference colloid for the conditions: in-plane and out-of-plane lipid mobility (labeled ρz), in-plane lipid mobility only (ρ), out-of-plane lipid mobility (z), and no lipid mobility (*two dashes*). The headgroups have a local mobility with respect to their tails. The arrow indicates the smallest membrane-colloid separation possible for the systems without out-of plane lipid mobility ($s = -3.88$ Å).

First, the two potential of mean force curves for membranes with in-plane lipid mobility display strong attractive regions, whereas the corresponding curves without in-plane lipid mobility possess a maximum attraction of $1kT$. Hence, surface polarization is more important than protrusions in establishing an attraction between a charged colloid and the net neutral membrane composed of cationic and anionic lipids. Nevertheless, the influence of protrusions is still significant. Since it matters whether polarization is present or not, we will consider the two cases separately.

When comparing membranes with in-plane lipid mobility and with in-plane and out-of-plane lipid mobility (cf. curves labeled ρ and ρz), we observe that, for the latter system, 1), the minimum of the potential of mean force is half as deep and appears at a longer separation ($s \approx 3$ Å instead of $s = -1$ Å); 2), at separations $s > 3$ Å the attraction is stronger; and 3), at short separations, the repulsion increases more weakly upon decreasing s. The first observation is obviously related to the entropic repulsion that appears when the protrusions are restricted for s ≤ 5 Å (cf. Fig. 3). At longer separations, the out-of-plane mobility has the opposite effect on the interaction; now this mobility enables the charged headgroups to be displaced toward the colloid and increases the favorable electrostatic interaction. The final observation follows from the fact that the lipids are able to yield (in the negative z direction) as the colloid penetrates more deeply in the membrane. Hence, lipid protrusion makes the potential of mean force more long-range, but the magnitude of the attraction near the minimum is smaller.

When the lipid in-plane mobility is absent, the effect of the out-of-plane lipid mobility is much smaller (cf. Fig. 9, curves z and *two dashes*). Observations 2) and 3) are still true, but the

variation of the associated free energies is much smaller. The long-range attraction appearing with protrusions is due to the different displacements of the cationic and anionic lipids, now with their checkerboard arrangement preserved (cf. discussion of Fig. 5). The weak minimum appearing in the absence of both the in-plane and out-of-plane lipid mobility originates from the local headgroup mobility.

Let us now evaluate how the presence of protrusions influences the polarization. Fig. 10 displays the relative surface charge polarization $\sigma_r(\rho)$ as a function of ρ at different membrane-colloid separations for the reference colloid with and without lipid out-of-plane mobility at separations $s = 1.4$ and 5.3 Å. It is seen that the presence of protrusions enhances the lipid polarization of the surface. This effect is stronger at the larger separation since the protrusions enable the headgroups to preserve some contact with the colloid (Fig. 6 *A*); without protrusions, the headgroup-colloid surface-to-surface separation is obviously 5.3 Å. It is noticeable that, at the shorter separation, the polarization at $\rho = 0$ is slightly stronger in the absence of protrusions. A rationale for this is that with protrusions it is more favorable to displace some anionic lipids near the colloid away from the colloid than to exchange them for cationic ones. This is corroborated by $Z_{ex} = 19.0$ and 15.9 obtained with and without protrusions, respectively, for $s = 1.4$ Å, and 18.2 and 10.6 obtained with and without protrusions, respectively, for $s = 5.3$ Å.

CONCLUSIONS

In a previous study, we observed that the details of the membrane strongly affect the adsorption of a polyion onto it. In particular, it was possible to adsorb a polyelectrolyte onto an overall neutral membrane made of positive and negative charged headgroups if the headgroups were frozen in a disordered state or were allowed to move and adapt to the adsorbing polyelectrolyte (11).

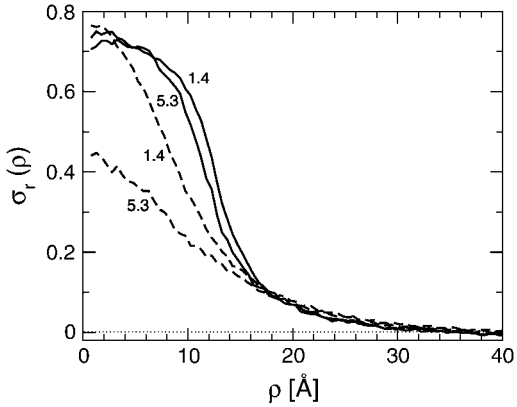

FIGURE 10 Relative surface charge polarization $\sigma_r(\rho)$ as a function of ρ for the reference colloid at the indicated membrane-colloid separations (Å) for the conditions characterized by in-plane and out-of-plane mobilities (*solid curves*) and in-plane mobility only (*dashed curves*).

In this study, we developed the model further to include protrusion of the lipids perpendicular to the membrane, as well as the in-plane translation of the lipids. It was found that the protrusion of individual headgroups causes undulations that propagate throughout the membrane. The undulations were slightly larger when the headgroups were neutral than when they were charged. The dispersion of the headgroups was found to be in good agreement with that calculated from the capillary wave theory and was also similar to values determined experimentally or by computer simulations of similar systems.

When an uncharged colloid was placed in the vicinity of the membrane, a short-range repulsion was observed that deflected the membrane away from the colloid to preserve the protrusions. Conversely, when the colloid was charged, the headgroups moved toward it; on average, the positive headgroups occupied a position closer to the colloid and the anionic headgroups were placed farther away from the colloid. The fact that the headgroups were allowed to embrace the colloid and therefore increase the contact area induced an increase in the polarization of the headgroups, as compared to similar systems without protrusions. Calculations of the potential of mean force showed that in the presence of protrusions the attractive potential is more long-range but has a smaller magnitude at short separations.

This work was supported by grants from a European Union Research Training Network, CIPSNAC (contract No. MRTN-CT-2003-504932), and the Fundação para a Ciência e Tecnologia, Portugal (SFRH/BPD/24203/2005). The use of the computing resources of Lunarc, the Center for Scientific and Technical Computing at Lund University, is gratefully acknowledged.

REFERENCES

1. Cockburn, J. J. B., N. G. A. Abrescia, J. M. Grimes, G. C. Sutton, J. M. Diprose, J. M. Benevides, G. J. Thomas, J. K. H. Bamford, D. H. Bamford, and D. I. Stuart. 2004. Membrane structure and interactions with protein and DNA in bacteriophage PRD1. *Nature*. 432:122–125.
2. Maier, B., and J. O. Radler. 2000. DNA on fluid membranes: a model polymer in two dimensions. *Macromolecules*. 33:7185–7194.
3. Leal, C., D. Sandström, P. Nevsten, and D. Topgaard. 2008. Probing local and translational dynamics in DNA-lipid assemblies monitored by solid-state and diffusion NMR. *Biochim. Biophys. Acta*. 1778:214–228.
4. Denisov, G., S. Wanaski, P. Luan, M. Glaser, and S. McLaughlin. 1998. Binding of basic peptides to membranes produces lateral domains enriched in the acidic lipids phosphatidylserine and phosphatidylinositol 4,5-bisphosphate: an electrostatic model and experimental results. *Biophys. J.* 74:731–744.
5. May, S., D. Harries, and A. Ben-Shaul. 2000. Lipid demixing and protein-protein interactions in the adsorption of charged proteins on mixed membranes. *Biophys. J.* 79:1747–1760.
6. Harries, D., S. May, and A. Ben-Shaul. 2002. Adsorption of charged macromolecules on mixed fluid membranes. *Colloid Surface A*. 208: 41–50.
7. Hinderliter, A., and S. May. 2006. Cooperative adsorption of proteins onto lipid membranes. *J. Phys. Condens. Matter*. 18:S1257–S1270.
8. Mbamala, E. C., A. Ben-Shaul, and S. May. 2005. Domain formation induced by the adsorption of charged proteins on mixed lipid membranes. *Biophys. J.* 88:1702–1714.

9. Shi, X.-Q., and Y.-Q. Ma. 2007. Effective attraction interactions between like-charge macroions bound to binary fluid lipid membranes. *J. Chem. Phys.* 126:125101.
10. Fleck, C., R. R. Netz, and H. H. von Grunberg. 2002. Poisson-Boltzmann theory for membranes with mobile charged lipids and the pH-dependent interaction of a DNA molecule with a membrane. *Biophys. J.* 82:76–92.
11. Dias, R. S., A. A. C. C. Pais, P. Linse, M. G. Miguel, and B. Lindman. 2005. Polyion adsorption onto catanionic surfaces. A Monte Carlo study. *J. Phys. Chem. B.* 109:11781–11788.
12. Tzlil, S., and A. Ben-Shaul. 2005. Flexible charged macromolecules on mixed fluid lipid membranes: theory and Monte Carlo simulations. *Biophys. J.* 89:2972–2987.
13. Israelachvili, J. N., and H. Wennerstrom. 1992. Entropic forces between amphiphilic surfaces in liquids. *J. Phys. Chem.* 96:520–531.
14. Israelachvili, J. N., and H. Wennerstrom. 1990. Hydration or steric forces between amphiphilic surfaces. *Langmuir.* 6:873–876.
15. Cevc, G. 1991. Hydration force and the interfacial structure of the polar surface. *J. Chem. Soc., Faraday Trans.* 87:2733–2739.
16. Hoyrup, P., T. H. Callisen, M. O. Jensen, A. Halperin, and O. G. Mouritsen. 2004. Lipid protrusions, membrane softness, and enzymatic activity. *Phys. Chem. Chem. Phys.* 6:1608–1615.
17. Halperin, A., and O. G. Mouritsen. 2005. Role of lipid protrusions in the function of interfacial enzymes. *Eur. Biophys. J.* 34:967–971.
18. Gao, H. J., W. D. Shi, and L. B. Freund. 2005. Mechanics of receptor-mediated endocytosis. *Proc. Natl. Acad. Sci. USA.* 102:9469–9474.
19. Sun, S. X., and D. Wirtz. 2006. Mechanics of enveloped virus entry into host cells. *Biophys. J.* 90:L10–L12.
20. Deserno, M. 2004. When do fluid membranes engulf sticky colloids? *J. Phys. Condens. Matter.* 16:S2061–S2070.
21. Deserno, M. 2004. Elastic deformation of a fluid membrane upon colloid binding. *Phys. Rev. E.* 69:031903.
22. Deserno, M., and T. Bickel. 2003. Wrapping of a spherical colloid by a fluid membrane. *Europhys. Lett.* 62:767–773.
23. Fleck, C. C., and R. R. Netz. 2004. Electrostatic colloid-membrane binding. *Europhys. Lett.* 67:314–320.
24. Schiessel, H. 1998. Bending of charged flexible membranes due to the presence of macroions. *Eur. Phys. J. B.* 6:373–380.
25. Jensen, M. O., and O. G. Mouritsen. 2004. Lipids do influence protein function: the hydrophobic matching hypothesis revisited. *Biochim. Biophys. Acta.* 1666:205–226.
26. Sperotto, M. M., S. May, and A. Baumgaertner. 2006. Modelling of proteins in membranes. *Chem. Phys. Lipids.* 141:2–29.
27. Brannigan, G., and F. L. H. Brown. 2006. A consistent model for thermal fluctuations and protein-induced deformations in lipid bilayers. *Biophys. J.* 90:1501–1520.
28. Nielsen, S. O., B. Ensing, V. Ortiz, P. B. Moore, and M. L. Klein. 2005. Lipid bilayer perturbations around a transmembrane nanotube: a coarse grain molecular dynamics study. *Biophys. J.* 88: 3822–3828.
29. Noguchi, H., and M. Takasu. 2002. Adhesion of nanoparticles to vesicles: a Brownian dynamics simulation. *Biophys. J.* 83:299–308.
30. Reynwar, B. J., G. Illya, V. A. Harmandaris, M. M. Muller, K. Kremer, and M. Deserno. 2007. Aggregation and vesiculation of membrane proteins by curvature-mediated interactions. *Nature.* 447:461–464.
31. Nilsson, U., B. Jonsson, and H. Wennerstrom. 1993. Catanionic amphiphilic layers: a Monte Carlo simulation study of surface forces. *J. Phys. Chem.* 97:5654–5660.
32. Jönsson, B., and H. Wennerström. 1981. Thermodynamics of ionic amphiphile-water systems. *J. Colloid Interface Sci.* 80:482–496.
33. Parsegian, V. A. 1966. Theory of liquid-crystal phase transitions in lipid + water systems. *Trans. Faraday Soc.* 62:848–860.
34. Jönsson, B., and H. Wennerström. 1987. Phase-equilibria in a 3-component water-soap-alcohol system: a thermodynamic model. *J. Phys. Chem.* 91:338–352.
35. Evans, D. F., D. J. Mitchell, and B. W. Ninham. 1984. Ion binding and dressed micelles. *J. Phys. Chem.* 88:6344–6348.
36. Allen, M. P., and D. J. Tildesley. 1987. Computer Simulations of Liquids. Clarendon, Oxford.
37. Arnold, A., J. de Joannis, and C. Holm. 2002. Electrostatics in periodic slab geometries I. *J. Chem. Phys.* 117:2496–2502.
38. Linse, P. 2004. MOLSIM, Version 4.0.0, Lund University, Sweden.
39. Linse, P. 2002. Mean force between like-charged macroions at high electrostatic coupling. *J. Phys. Condens. Matter.* 14:13449–13467.
40. Davis, H. T. 1977. Capillary waves and the mean field theory of interfaces. *J. Chem. Phys.* 67:3636–3641.
41. Kucerka, N., S. Tristram-Nagle, and J. F. Nagle. 2006. Structure of fully hydrated fluid phase lipid bilayers with monounsaturated chains. *J. Membr. Biol.* 208:193–202.
42. Kucerka, N., Y. F. Liu, N. J. Chu, H. I. Petrache, S. T. Tristram-Nagle, and J. F. Nagle. 2005. Structure of fully hydrated fluid phase DMPC and DLPC lipid bilayers using X-ray scattering from oriented multilamellar arrays and from unilamellar vesicles. *Biophys. J.* 88:2626–2637.
43. Nagle, J. F., R. T. Zhang, S. Tristram-Nagle, W. J. Sun, H. I. Petrache, and R. M. Suter. 1996. X-ray structure determination of fully hydrated Lα phase dipalmitoylphosphatidylcholine bilayers. *Biophys. J.* 70: 1419–1431.
44. McIntosh, T. J., S. Advani, R. E. Burton, D. V. Zhelev, D. Needham, and S. A. Simon. 1995. Experimental tests for protrusion and undulation pressures in phospholipid bilayers. *Biochemistry.* 34:8520–8532.
45. Lindahl, E., and O. Edholm. 2000. Spatial and energetic-entropic decomposition of surface tension in lipid bilayers from molecular dynamics simulations. *J. Chem. Phys.* 113:3882–3893.
46. Kaznessis, Y. N., S. T. Kim, and R. G. Larson. 2002. Simulations of zwitterionic and anionic phospholipid monolayers. *Biophys. J.* 82: 1731–1742.
47. Doxastakis, M., A. K. Sum, and J. J. de Pablo. 2005. Modulating membrane properties: the effect of trehalose and cholesterol on a phospholipid bilayer. *J. Phys. Chem. B.* 109:24173–24181.
48. Suits, F., M. C. Pitman, and S. E. Feller. 2005. Molecular dynamics investigation of the structural properties of phosphatidylethanolamine lipid bilayers. *J. Chem. Phys.* 122:244714.
49. Kik, R. A., F. A. M. Leermakers, and J. M. Kleijn. 2005. Molecular modeling of lipid bilayers and the effect of protein-like inclusions. *Phys. Chem. Chem. Phys.* 7:1996–2005.